Mining, Metallurgy & Exploration (2020) 37:481–492
https://doi.org/10.1007/s42461-019-00167-8

Estimation of Grinding Time for Desired Particle Size Distribution and for Hematite Liberation Based on Ore Retention Time in the Mill

Harish Hanumanthappa[1] · Harsha Vardhan[1] · Govinda Raj Mandela[1] · Marutiram Kaza[2] · Rameshwar Sah[2] · Bharath Kumar Shanmugam[1]

Received: 27 August 2019 / Accepted: 16 December 2019 / Published online: 3 January 2020

Abstract
Iron ores obtained from different sources differ in their chemical and physical properties. These variations make the process of grinding a difficult task. The work carried out in this context focuses on three different samples of iron ore, viz., high silica high alumina, low silica high alumina, and low silica low alumina. The grinding process for all the three iron ores is carried out individually in Bond's ball mill and the total retention time taken by each iron ore sample is calculated. The present investigation focuses on utilizing the calculated retention time of the iron ore as a standard grinding reference time to the laboratory ball mill for optimizing the grinding time of each ore. The desired P_{80} (150 μm) with an acceptable range of hematite liberation (> 75%) was obtained in the laboratory ball mill after reducing 6 min from the total retention time taken in the Bond ball mill.

Keywords Particle size distribution (PSD) · Retention time · Comminution · Characterization studies

1 Introduction

Ball mills are progressively used to grind the ores for particle size reduction and to liberate valuable minerals from the ores. The grinding of ore is a highly energy-intensive process [1–4]. In this process, the size of the particle obtained depends on the energy consumption of the ball mill. The major challenge encountered in the process of iron ore grinding is to maintain the desired product particle size distribution (PSD) with sufficient liberation of valuable minerals. The demand for desired particle size with maximum liberation of valuables is increasing, particularly in the last phase of the grinding, for primary feed preparation for the making of pellets.

There are many tests for determining grindability. The most commonly used test is the Bond ball mill (BBM). It enables the installation of a plant scale ball mill [5]. The Bond work index test is used to measure the energy required for the desired particle size reduction and for designing new circuits for comminution [5]. The Bond work index is commonly agreed as a grindability factor for ores in order to relate different material compositions [6]. Several works related to the strength of the Bond test with respect to the grindability factor are discussed [7–13].

The Bond test analysis specifies that one of the vital parameters for computing work indices is PSD [9]. In this sense, the standard Bond test procedure is used to analyze PSD in terms of F_{80} and P_{80} parameters.

It is well-recognized in conventional grinding that PSD and effective liberation of valuable materials from the gangue, which occurs at different particle sizes, depends mainly on the properties of the ore being ground. The liberation properties of the valuables depend on its chemical and physical composition, which helps in the selection of the processing methods enabling effective utilization of the iron ore [14–17]. The size reduction and liberation of the particles are accomplished by the grinding process [18]. It is often hard to control the PSD in the end product. In a combined mineral processing, the liberation of valuables assists as a link between the grinding and the separation by creating particle structure information for the ground products [19]. However, it has been documented that there is an

✉ Harish Hanumanthappa
hari.harish86@gmail.com

[1] Department of Mining Engineering, National Institute of Technology Karnataka, Surathkal, Mangalore 575025, India

[2] R & D and SS, JSW Steel Limited, Vijayanagar Works, P.O. Vidyanagar, Ballari, Karnataka 583275, India

uneven breakage in ores, which leads to uneven liberation of minerals [20, 21].

The production of the desired PSD for different source of ores is difficult whenever a ball mill operates at constant operating parameters [18]. The variation in PSD might be due to the different trends in the mineralogical and physical composition of a representative sample from various sources [22]. The mineralogical characterization is considered as a vital tool governing the process of grinding and liberation-related productivity improvement. The study of microstructure and mineralogy plays a significant role in understanding mineral behavior at different stages of the grinding process [23].

In the present scenario, characterization studies were being carried out pertaining to ore liberation and associations of mineral phases, grain size, and textural features by using automated microscopic techniques [24–26]. Improvement of computerized microscopic systems has now made it possible to scan the mineral components of different types of ores [27]. An ore can be characterized by QEMSCAN based on the presence of minerals and their association with respect to every single mineral [28, 29]. The analysis rate of QEMSCAN is rapid to determine the mineralogy and individual ore particle size measurement. The QEMSCAN analysis data consists of mineral association, the grain size of the minerals, and the phase of the minerals.

Along with different operating parameters of the mill and mineralogical characterization, the residence time distribution (RTD) of the mill also plays a very important role in the design of the ball mill circuit. Numerous studies have focused on RTD measurement with respect to solid flow effect, solid transport alongside the mill axis, and variation of ball mill diameter on RTD in the ball mill [30–32]. The different types of RTD measurement methods used were attainable region technique, one-parameter RTD model, and radioactive tracer [33–35].

However, from the literature survey, it was observed that PSD and size-by-size liberation in the fine grinding phase are not clear with a variation of grinding time [36–39]. Hence, the liberation of minerals from ores is still uncertain and conflicting, and this may be associated with the mineralogical textures of dissimilar ores. Furthermore, the difference in the relation between PSD and hematite liberation in the product size has not been specified clearly in earlier works.

The aim of the present study is to measure the total retention time of high silica high alumina (HSHA), low silica high alumina (LSHA), and low silica low alumina (LSLA) iron ore samples using a new approach. Also, the measured total retention time of each ore as a standard reference grinding time was used to achieve the desired P_{80} passing percentage of 150 μm with an acceptable range of hematite liberation (> 75%) from iron ores for the pellet making process by using BBM and laboratory ball mill (LBM).

2 Experimental Method

2.1 Samples

In the present study, iron ore of three different chemical compositions was selected from Karnataka region. These samples are typical raw materials used in JSW Steel, Ballari Pellet Plant, to produce pellets. The selected iron ores are mainly classified into three groups based on the percentage of silica and alumina present in each sample, as shown in Table 1. The chemical composition of the selected iron ore samples is shown in Table 2. In the crushing machine, all the three iron ore samples were crushed to − 3 mm and analyzed for the desired P_{80} passing (− 150 μm) and percentage of hematite liberated in the three feed iron ore samples. The – 150-μm feed size fractions were selected to determine the nominal degree of hematite liberation from the representative HSHA, LSHA, and LSLA feed iron ore samples. The crushed – 3-mm iron ore samples were used as feed to the BBM and LBM. The processing flow sheet is represented in Fig. 1.

2.2 Grinding Studies

Two kinds of mills, BBM and LBM, were used to achieve the desired P_{80} passing percentage of 150 μm with an acceptable range of hematite liberation (> 75%) at optimum grinding time. The BBM is a standard ball mill having a length and diameter of 300 mm × 300 mm with smooth liner as shown in Fig. 2. A rotating drum is attached to a gearbox and has adjustable speed knob. The number of steel balls and the weight of the balls are selected according to Bond's standard procedure [40].

A bench test was developed for dry grinding to determine the Bond work index and to know the PSD and hematite liberation in all the three iron ore product samples obtained from the BBM. For each iron ore sample, 700 cc of feed was weighed and added into the BBM. The BBM was set for 100 revolutions in the first iteration. The product from the mill was withdrawn after completion of 100 revolutions. The product was then screened and analyzed. Oversized fractions were added back into the mill (as it is a closed-circuit operation). The amount of fresh feed added to the mill is equal to the amount of undersized fractions produced in the first iteration. The number of revolutions for the second iteration is determined based on Bond's standard test procedure [40]. The experiments were continued for a minimum of five consecutive iterations until the net grams per revolution became constant.

A new method was adopted to measure the total retention time taken by each ore in the BBM. The

Table 1 Percentage variation of silica and alumina by weight in iron ore

Sl. no.	Type of ore	Silica% by wt. in iron ore	Alumina% by wt. in iron ore
1	HSHA iron ore	> 4.5	> 3.5
2	LSHA iron ore	< 4.5	> 3.5
3	LSLA iron ore	< 4.5	< 3.5

retention time of the ore in the mill is measured based on the total number of revolutions taken by each ore to produce 250% of circulating load. The number of revolutions for each trail is set to the BBM based on Bond's procedure. For each trial, the set number of revolutions is recorded and represented as R_1, R_2, R_3, R_4, …..R_n. The total number of revolutions taken by each ore sample in the BBM is calculated using Eq. 1.

$$R = R_1 + R_2 + R_3 + R_4 + \ldots\ldots + R_{n-1} + R_n \quad (1)$$

The total retention time taken by the BBM for each iron ore sample is given by Eq. (1).

$$T = \frac{\text{Total number of revolution taken by BBM to produce 250\%circulating load for each iron ore sample}}{number\ of\ revolutions\ per\ minute} \quad (2)$$

The standard equation used to determine the work index is given in Eq (3).

$$BWI = \frac{48.95}{A^{0.23}\ \text{x}\ G_{bp}^{0.82}\left(\frac{10}{\sqrt{P_{80}}} - \frac{10}{\sqrt{F_{80}}}\right)} kWh/t \quad (3)$$

where F_{80} is 80% passing particle size of the feed in μm, P_{80} is 80% passing particle size of the final grinding cycle product in μm, A is the mesh size of the test in m, and G_{bp} is the grindability of the undersized product produced per mill revolution (g/rev).

The same feed samples of HSHA, LSHA, and LSLA used in the BBM are used as feed for the LBM. The test mill has an internal diameter of 500 mm, and it is 1000 mm long as shown in Fig. 3. In the LBM, the experiments were conducted based on the total retention time taken by HSHA, LSHA, and LSLA iron ore samples in the BBM. The LBM experiments were performed based on trial and error method, i.e., by reducing the total retention time obtained from BBM by 2 min, 4 min, and 6 min for the HSHA, LSHA, and LSLA samples, respectively.

For all the samples, the speed of the mill, feed to the mill, and media (balls) were kept constant. The only parameter, which varied in the LBM, was the grinding time. The grinding time of LBM in each case was changed by reducing 2 min from the total retention time taken to produce 250% circulating load in the BBM. After the completion of each experiment in the LBM, particle size analysis was carried out to identify the P_{80} passing percentage particle size fraction and percentage of liberation. The operations were repeated in the LBM for the HSHA, LSHA, and LSLA samples until the P_{80} passing particle size fraction of 150 μm was achieved.

Table 2 Chemical composition of iron ores

Sl. no.	Type of ore	Fe%	SiO_2%	Al_2O_3%	LOI%
1	HSHA iron ore	60.42	5.58	4.03	3.17
2	LSHA iron ore	59.51	3.21	4.71	5.09
3	LSLA iron ore	61.09	3.36	2.76	4.36

2.3 Techniques Used

Sieve analysis was carried out with the help of a Ro-Tap reciprocating mechanical sieve shaker to determine the percentage of the different grain sizes contained in the samples. The particle size analysis of the three iron ore feed samples is given in Fig. 4. It was observed from the feed analysis that 80% passing of the particles is of sizes below 2.5 mm, 2.4 mm, and 2.7 mm for the HSHA, LSHA, and LSLA iron ore samples, respectively. The density of all the three feed samples was determined using the Pycnometer. The particle density of the three feed samples varied from one another. The particle density of the feed sample was found to be 3.36 g/cm^3, 3.47 g/cm^3, and 3.52 g/cm^3 in HSHA, LSHA, and LSLA, respectively. The sink and float study was carried out to analyze the percentage of liberation of hematite in the grounded ore sample using organic liquid with a density of 3.3 g/cm^3 (diiodomethane). About − 150 μm size fractions were selected to determine the nominal degree of liberation of the representative HSHA, LSHA, and LSLA iron ore samples.

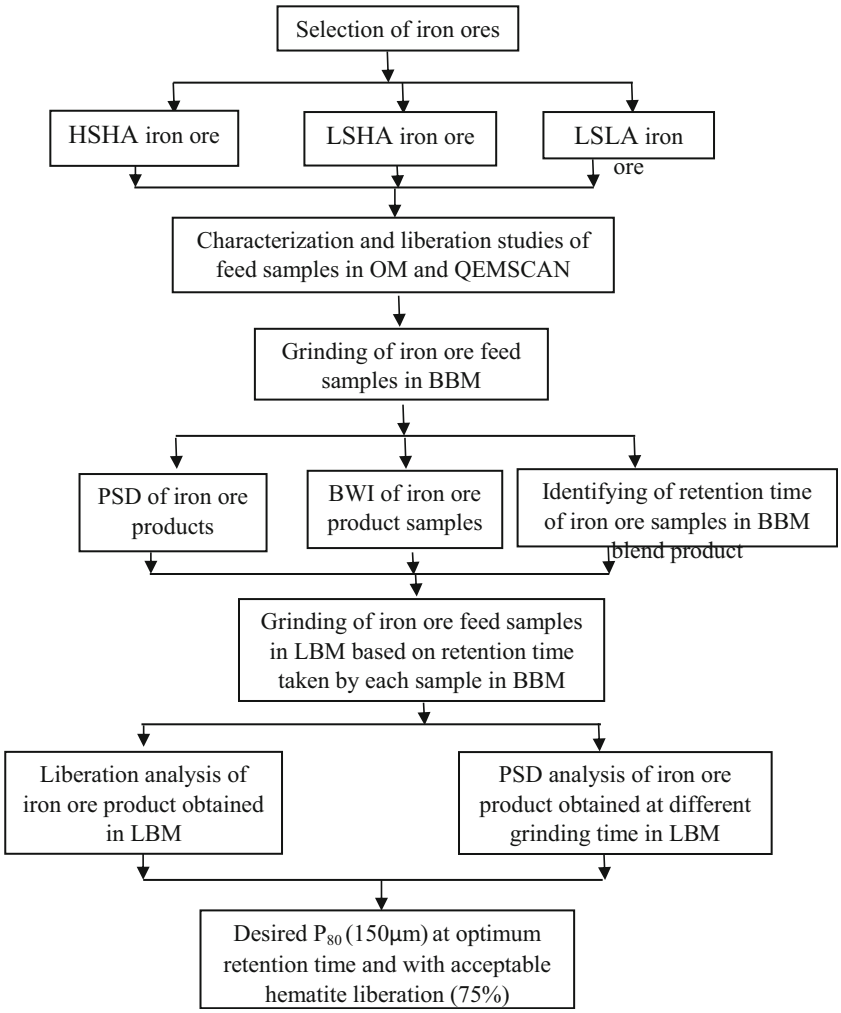

Fig. 1 Process flow sheet to achieve the desired P_{80} (150 μm) at optimum retention time and with acceptable hematite liberation

The micrographs and degree of hematite liberation from the iron ore feed samples were analyzed and compared using the optical microscope (model Leica DMLP) and the QEMSCAN (Quanta FEG 650).

For the liberation study, − 150-μm particles were screened from the feed and product samples. For both the feed and product samples, polished specimens were prepared and analyzed in an optical microscope. The volumetric grade in the valuable minerals is statistically equivalent to the surface concentration and is expressed as given in Eq. 4.

$$T\% = \frac{Total\ area\ of\ valuable\ minerals}{Total\ area\ of\ particles} * 100 \quad (4)$$

The following Eq 5. ratio expresses the apparent degree of liberation of the sample of particles represented in a section of the sample.

$$L\% = \frac{Total\ are\ of\ valuable\ \text{minerals}}{Total\ are\ of\ mineralized\ particles} * 100 \quad (5)$$

3 Results and Discussion

3.1 Mineralogical Analysis of Feed Sample by Optical Microscopy and QEMSCAN

Figure 5 a, b, and c illustrate the mineralogical analysis of the feed samples of HSHA, LSHA, and LSLA using an optical microscope. The analysis derived through optical microscopy was measured with a discontinuous method. Figure 5 a and b represent HSHA and LSHA samples with a significant portion of hematite and are majorly distributed in spheroid form. In addition to this, some finer tubular structures of hematite are also observed in the optical microscopy. However, a major portion of HSHA is composed of Fe Ox-Al silicate interphase and goethite. The LSLA sample consists of major portions of hematite, and it is well-distributed in tubular and spheroid form, whereas LSHA samples include a minor part of limonite and kaolinite as shown in Fig. 5c. The gangue minerals in both LSHA and HSHA are majorly distributed in quartz form and other gangue minerals such as kaolinite and alumina are distributed separately from the quartz.

Fig. 2 Bond's ball mill

Figure 6 a, b, and c show the mineralogical analysis of the feed samples of HSHA, LSHA, and LSLA using the QEMSCAN Quanta FEG 650. The report obtained from the QEMSCAN was three major selections of field image, bulk mineral analysis (BMA), and particle mineral analysis (PMA). In the samples, HSHA and LSHA of Fig. 6 a and b, respectively, the major quantified phase is hematite. From Fig. 6c, in the LSLA sample, most of the quartz is present in the bulk phase, which can be liberated easily by controlled grinding. In the samples of HSHA and LSHA, the quartz phase has a high proportion of hematite in composite form, and hence, the removal of gangue material from the hematite will require intensive grinding.

3.2 Grinding and Liberation Analysis of HSHA, LSHA, and LSLA Products Obtained from BBM and LBM

The grinding studies were conducted based on Bond's standard procedure to determine Bond's work index and retention time using the BBM. The effect of retention time on PSD and the liberation of hematite from the iron ore for all the samples were analyzed.

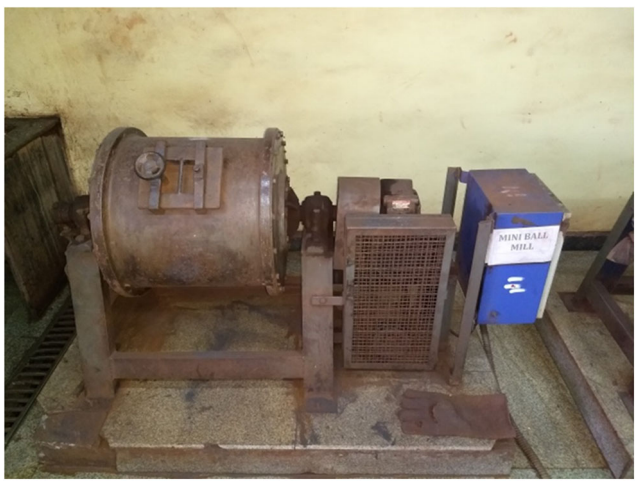

Fig. 3 Laboratory ball mill

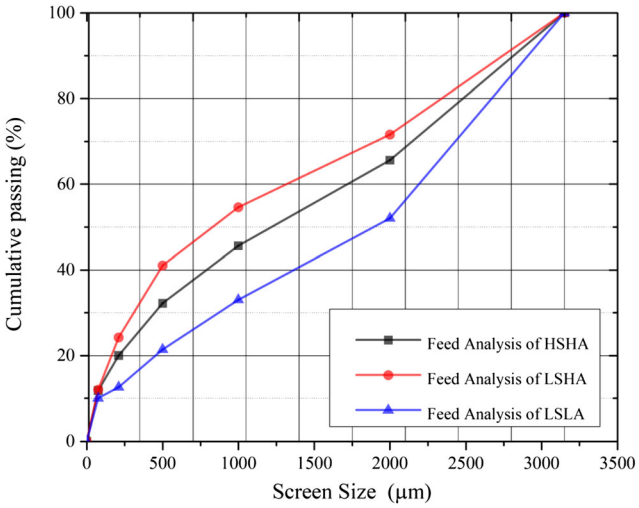

Fig. 4 Particle size analysis of HSHA, LSHA, and LSLA feed samples

The grinding studies in the LBM for all the iron ore samples were carried out based on the BBM total retention time taken for each representative sample obtaining 80% passing of the desired particle size fraction of 150 μm. This study was conducted with an acceptable range of hematite liberation, and the results are analyzed and discussed in the following sections.

3.2.1 Effect of Retention Time on Passing Percentage of P_{80} Particle Size in HSHA, LSHA, and LSLA

In this section, the influence of milling time condition on the P_{80} passing percentage of HSHA, LSHA, and LSLA products produced during BBM and LBM was investigated. In the present work, one cumulative weight product passing size of 80% was specified to examine the fineness of the ground PSD of the product for different grinding conditions. The comparison of PSD of a ground product of HSHA, LSHA, and LSLA with varying grinding times of BBM and LBM is shown in Figs. 7, 8, and 9, respectively.

From Table 3, the retention time taken for HSHA, LSHA, and LSLA from BBM was 16 min, 13 min, and 12 min. For HSHA, LSHA, and LSLA, the respective BWI was 12.8 kWh/t, 10.2 kWh/t, and 8.5 kWh/t and the P_{80} passing percentage was 72 μm, 60 μm, and 48 μm. But the desired passing percentage of 150 μm for a confined retention time was not achieved in the case of BBM. Hence, the BBM grinding behavior of HSHA, LSHA, and LSLA was used in the LBM by considering retention times of 16 min, 13 min, and 12 min, respectively. By trial and error method, from Table 4, the grinding time of 14 min, 12 min, and 10 min was considered for HSHA, and the P_{80} passing percentage was 96 μm, 130 μm, and 168 μm respectively. Whereas, in the case of LSHA, with the grinding time of 11 min, 9 min, and 7 min, the P_{80} passing percentage was

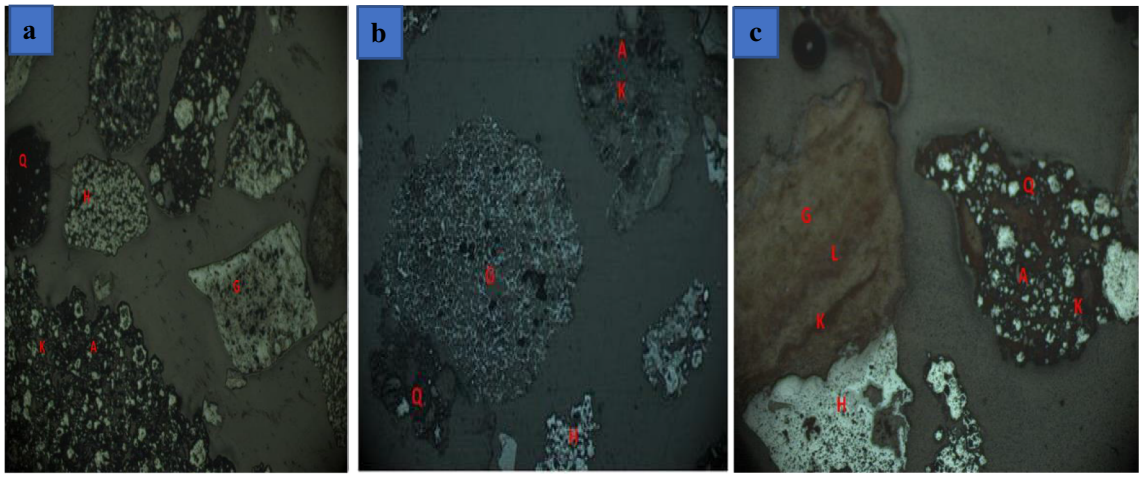

Fig. 5 Optical microscope photos for feed samples of **a** HSHA, **b** LSHA, and **c** LSLA

87 μm, 119 μm, and 152 μm, respectively. Similarly, in the case of LSLA, with the grinding time of 10 min, 8 min, and 6 min, the P_{80} passing percentage was 75 μm, 100 μm, and 140 μm, respectively.

When compared with mineralogical and grinding parameters, it can be found that the higher the weight percentage of silica and alumina (SiO_2 is > 4.5% and Al_2O_3 > 3.5%), the higher is the P_{80} passing size of the grinding product (and therefore, the harder it is to grind). Also, the lower the weight percentage of the silica and alumina (SiO_2 is < 4.5% and Al_2O_3 < 3.5%), the lower is the P_{80} passing size of the grinding product. This indicates that the presence of alumina and silica in the iron ore affects the grinding parameters of the ore. It is also clear that to obtain the desired percentage of P_{80} passing particle size in HSHA takes high grinding time compared with LSHA and LSLA, since the percentage of alumina and silica in HSHA is higher compared with that in LSHA and LSLA.

In comparison, the total retention time taken by each ore in the BBM is higher than the required grinding time of the ore to produce the desired PSD. The desired P_{80} is obtained after reducing 6 min from the retention time taken by each ore in the BBM. This method of controlling the retention time of the ore may save energy consumption by the mills. Finally, the optimum desired P_{80} passing (150 μm) percentage for HSHA, LSHA, and LSLA was 168 μm, 152 μm, and 140 μm, respectively, and is shown in Figs. 7, 8, and 9, respectively.

3.2.2 Effect of Retention Time on the Degree of Hematite Liberation in HSHA, LSHA, and LSLA

Figures 10a, 11a, and 12a present the optical microscope images of the liberated hematite of HSHA (retention time of 16 min), LSHA (retention time of 13 min), and LSLA (retention time of 12 min) obtained in the BBM. From Fig. 10a, hematite liberation is higher compared with LSHA and LSLA, as shown in Figs. 11a and 12a. This is because most of the hematite particles are in a liberated state in the feed samples and most of the quartz are present in the bulk phase, which can be liberated easily from the locked hematite as shown in Figs. 5c and 6c. But in the case of HSHA and LSHA, the hematite particles were locked in quartz as finer tubular structures in feed samples and required intensive grinding to be liberated as shown in Figs. 5a, b 6a, b. Hence, the liberation of hematite in the LSLA product sample is higher than that in the HSHA and LSHA product samples.

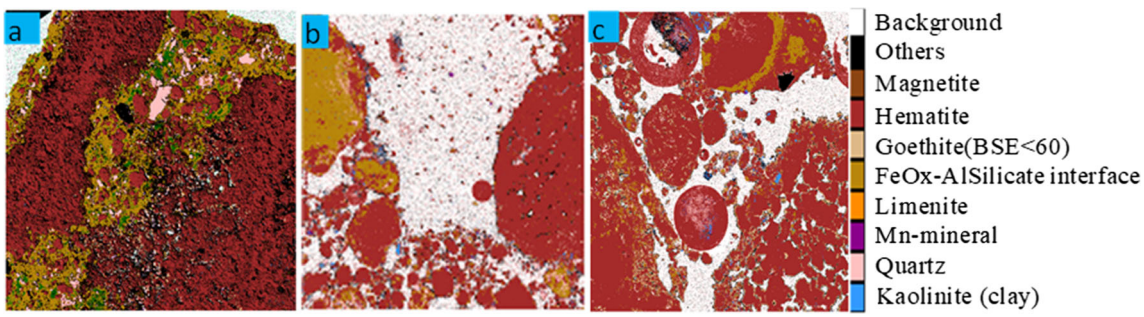

Fig. 6 QEMSCAN photos for feed samples of **a** HSHA, **b** LSHA, and **c** LSLA

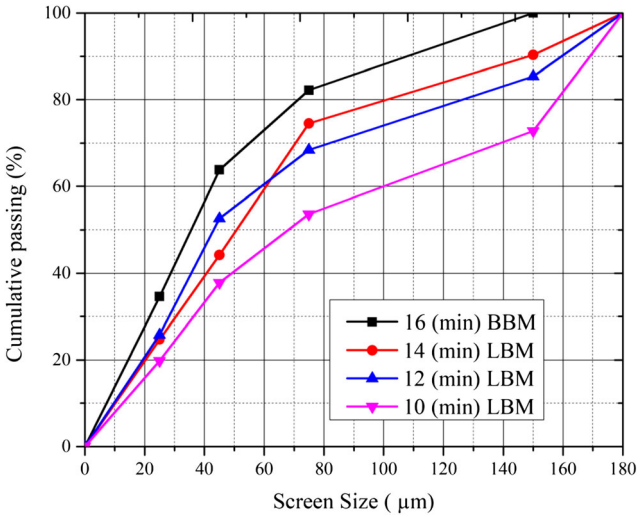

Fig. 7 Particle size analysis for HSHA product sample

The optical microscope analysis suggested that for HSHA, LSHA, and LSLA, the hematite liberation was 85%, 87%, and 93%, respectively, as shown in Table 3. However, the liberation of hematite in all the cases was well within the acceptable range (> 75%) and the P_{80} passing of all the three samples was very fine (72 μm, 60 μm, and 48 μm). The grinding results indicated that the desired P_{80} passing of 150-μm particles was not achieved for all the three types of the iron ore samples. Hence, all the three iron ore samples were further ground in the LBM based on the BBM retention time.

Figures 10b, 11b, and 12b indicate the optical microscope images of the hematite liberation of 82% for HSHA at 14 min, 84% for LSHA at 11 min, and 90% for LSLA at 10 min, respectively, using the LBM. The hematite liberation in all the cases was well within the acceptable range (hematite liberation > 75%). The P_{80} passing for all three iron ore samples was 96 μm at 14 min, 87 μm at 11 min, and 75 μm at 10 min.

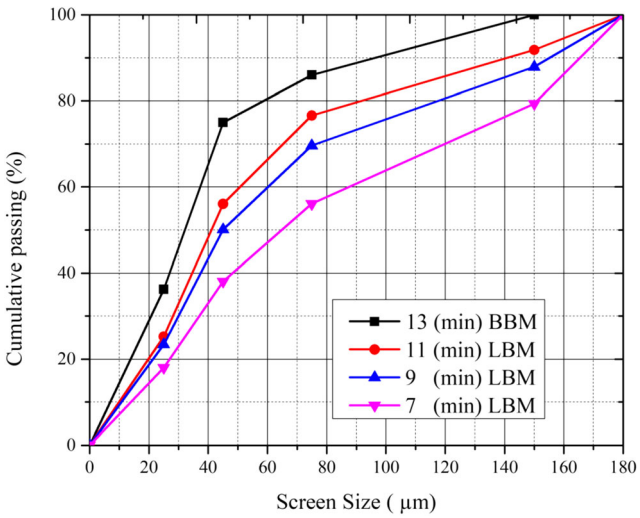

Fig. 8 Particle size analysis for LSHA product sample

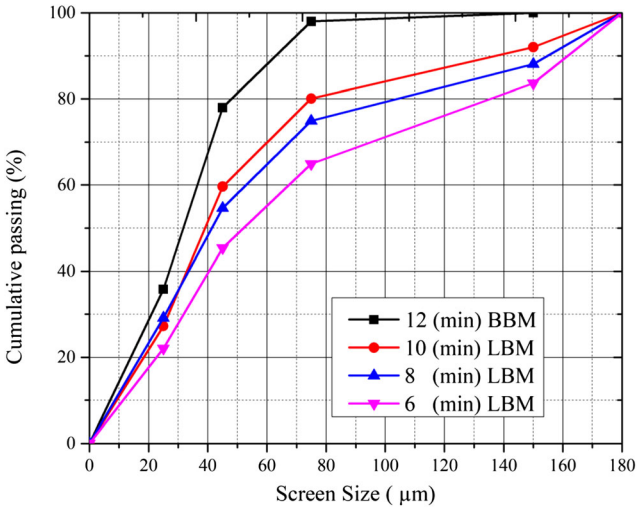

Fig. 9 Particle size analysis for LSLA product sample

Hence, the retention time of the LBM was further reduced to obtain the desirable P_{80} passing of 150-μm particles.

Figures 10c, 11c, and 12c indicate the optical microscope images of the hematite liberation of 79% for HSHA at 12 min, 81.5% for LSHA at 9 min, and 87% for LSLA at 8 min, respectively, using the LBM. The hematite liberation in all the cases was well within the acceptable range (hematite liberation > 75%). The P_{80} passing for all the three iron ore samples was 130 μm at 12 min, 119 μm at 9 min, and 100 μm at 8 min. Hence, the retention time of the LBM was further reduced to obtain the desirable P_{80} passing of 150-μm particles.

Figures 10d, 11d, and 12d indicate the optical microscope images of the hematite liberation of 78% for HSHA at 10 min, 80% for LSHA at 7 min, and 85% for LSLA at 6 min, respectively, using the LBM. The hematite liberation in all the cases was well within the acceptable range (hematite liberation > 75%). The P_{80} passing for all three iron ore samples was within the desired P_{80} passing of 150-μm particles.

On the other hand, Table 4 shows the influence of varying the grinding time on hematite liberation for HSHA, LSHA, and LSLA when ground in the LBM. The percentage of hematite liberated in all the three samples was less when ground for shorter duration. This may be due to the insufficiency of energy transmitted from the ball to the particles to crack the boundaries between the quartz and the oxidized iron minerals during the short period of grinding leading to the generation of a large number of "complex-type" locked particles without hematite liberation [41]. Due to this, mineral liberation, during short period grinding, is also very less. Also, with increasing milling time, the cracks between the quartz and the oxidized iron boundaries increase and propagate and get fractured to liberate the hematite from the locked quartz. Hence, the hematite liberation is higher with longer grinding period.

Table 3 Physical specification analysis of HSHA, LSHA, and LSLA using the Bond work index method

Sl. no.	Type of ore	F_{80} (μm)	P_{80} by BBM (μm)	BWI KWh/mt	Time for 250% circulating load (min)	Percentage of hematite liberated
1	HSHA	2500	72	12.8	16	85
2	LSHA	2400	60	10.2	13	87
3	LSLA	2700	48	8.5	12	93

Figure 13a–d shows the PSD, percentage of hematite liberation, and total grinding time taken for HSHA, LSHA, and LSLA iron ore samples using BBM and LBM. The P_{80} passing percentage for HSHA is higher compared with LSHA and LSLA. This is because the percentage of SiO_2 and Al_2O_3 is higher in the HSHA feed sample, which leads to a higher grinding time compared with LSHA and LSLA. It can be observed that with an increased grinding time, the P_{80} passing percentage for all the three samples decreases, but the hematite liberation in all the three samples increases. This indicates that the grinding time is directly proportional to hematite liberation, and it is inversely proportional to the P_{80} passing percentage.

The present work was used to find the total grinding retention time of each ore in the mill. Based on the total retention time of each ore, the optimum grinding time for each ore was identified to obtain the desired P_{80} passing particle size with acceptable hematite liberation. The results obtained after considering the standard reference retention time to the LBM were improved with respect to the desired P_{80} passing percentage of 150 μm and hematite liberation. Finally, the optimum grinding time required to achieve the desired P_{80} passing percentage of 150 μm with acceptable hematite liberation percentage (75%) for HSHA, LSHA, and LSLA was 10 min, 7 min, and 6 min, respectively. The new method followed in the present work to obtain the desired P_{80} passing percentage and hematite liberation from different types of iron ore can be implemented in a pellet plant to produce desire products for pellet feed making.

4 Conclusions

Three different samples of iron ore such as HSHA, LSHA, and LSLA were considered for the grinding studies. The characterization studies for the three iron ore samples were carried out using the optical microscopy and QEMSCAN after each stage of the grinding. The liberation studies based on the P_{80} passing percentage were discussed. BBM and LBM were used to perform the grinding. The BBM was used to calculate the total retention time taken for each ore in the mill. The estimated retention time of the iron ore in the mill was used as a standard grinding reference time to the LBM. The results obtained after considering the standard reference retention time to the LBM were improved with respect to the desired P_{80} passing percentage of 150 μm and hematite liberation. The optimum desired P_{80} passing (150 μm) percentage for HSHA, LSHA, and LSLA was 168 μm at 10 min, 152 μm at 7 min, and 140 μm at 6 min, respectively. The total retention time taken by each ore in the BBM was higher than the required grinding time of the ore to produce the desired PSD. The desired P_{80} was obtained in LBM after reducing 6 min from the total retention time taken by each ore in the BBM. By knowing the retention time of each ore, the grinding time for the desired P_{80} can be set, which will ultimately help to reduce the energy consumption by the mills. The new method

Table 4 Physical specification analysis of HSHA, LSHA, and LSLA using LBM

Sl. no.	Type of ore	F_{80} (μm)	P_{80} by LBM (μm)	Reduced grinding time in LBM (min)	Percentage of hematite liberated
1	HSHA	2500	96	14	82
			130	12	79
			168	10	78
2	LSHA	2400	87	11	84
			119	9	81.5
			152	7	80
3	LSLA	2700	75	10	90
			100	8	87
			140	6	85

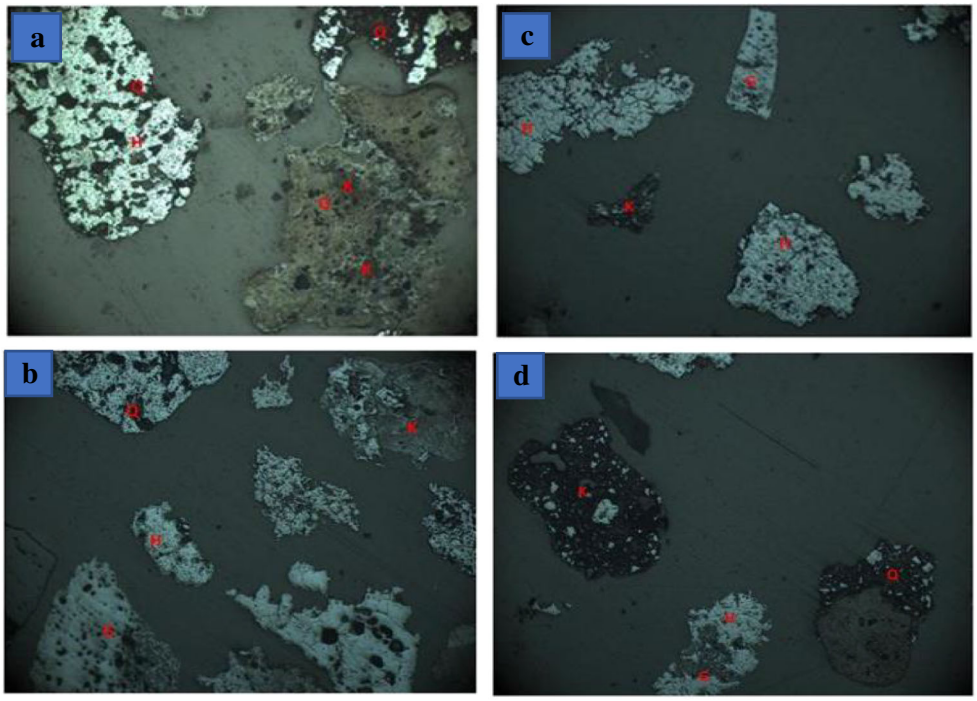

Fig. 10 **a** Optical microscopy of HSHA sink sample of size − 150 μm grounded for 16 min in BBM. **b**–**d** Optical microscopy of HSHA sink sample of size − 150 μm grounded for 14, 12, and 10 min in LBM

followed in the present work to obtain the desired P_{80} passing percentage and hematite liberation from different types of iron ore can be implemented in pellet plants to produce the desire products for pellet feed making.

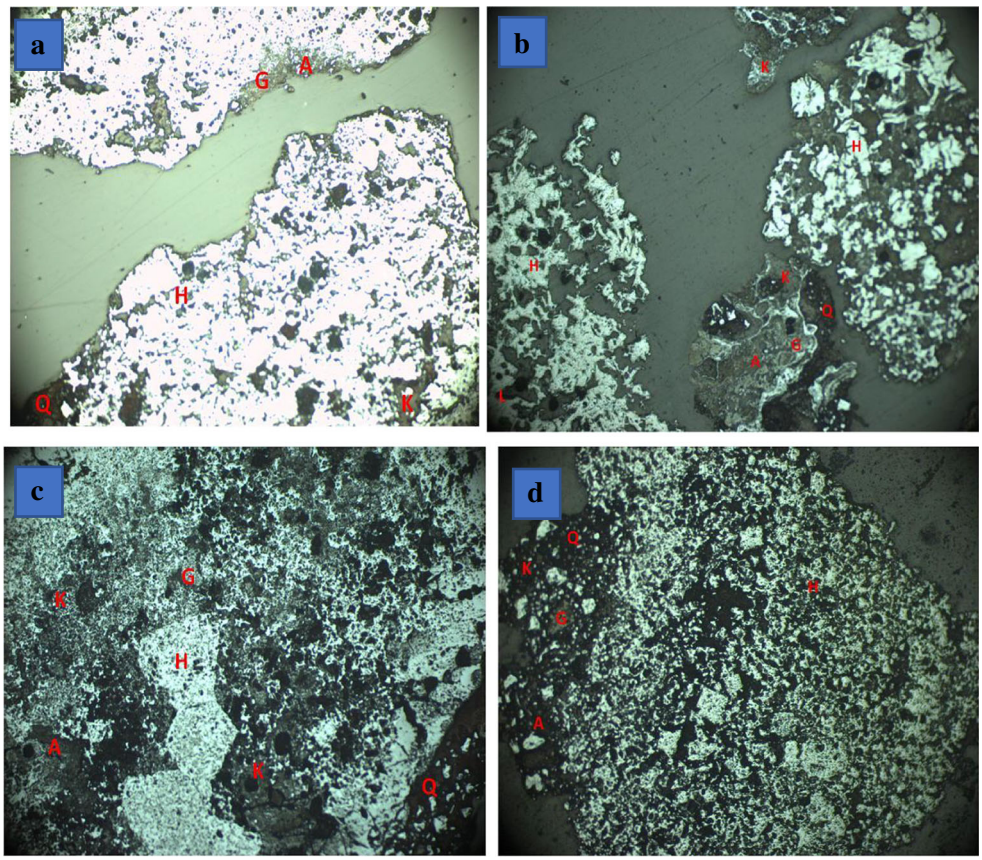

Fig. 11 **a** Optical microscopy of LSHA sink sample of size − 150 μm grounded for 13 min in BBM. **b**–**d** Optical microscopy of LSHA sink sample of size − 150 μm grounded for 11, 9, and 7 min in LBM

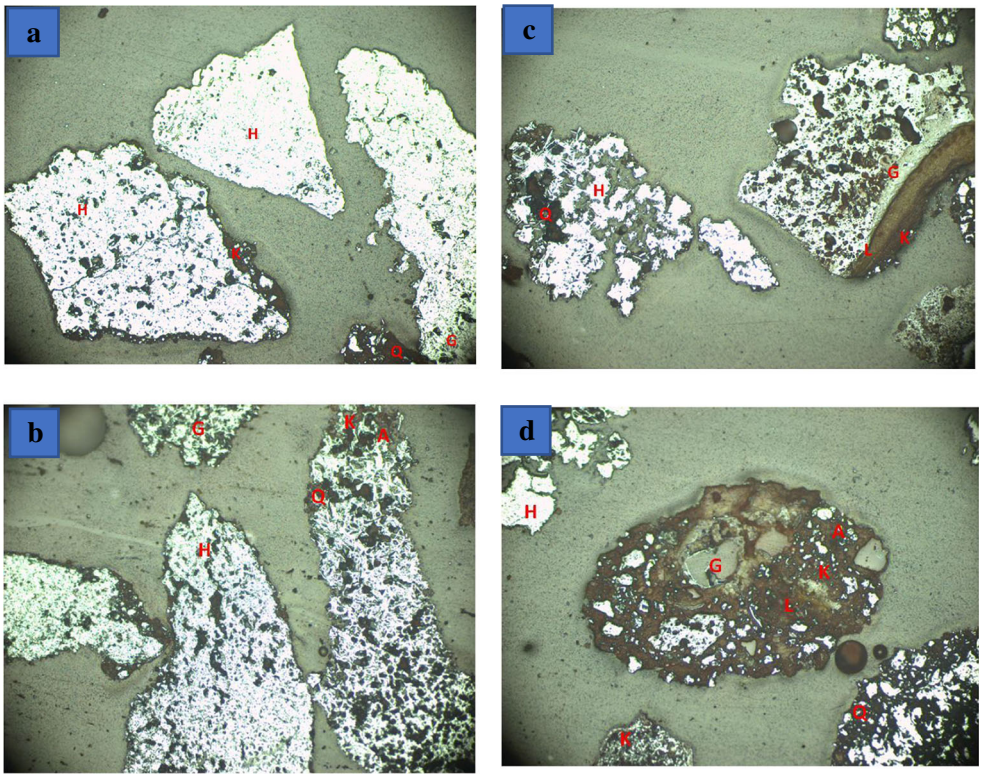

Fig. 12 **a** Optical microscopy of LSLA sink sample of size − 150 μm grounded for 12 min in BBM. **b**–**d** Optical microscopy of LSLA sink sample of size − 150 μm grounded for 10, 8, and 6 min in LBM

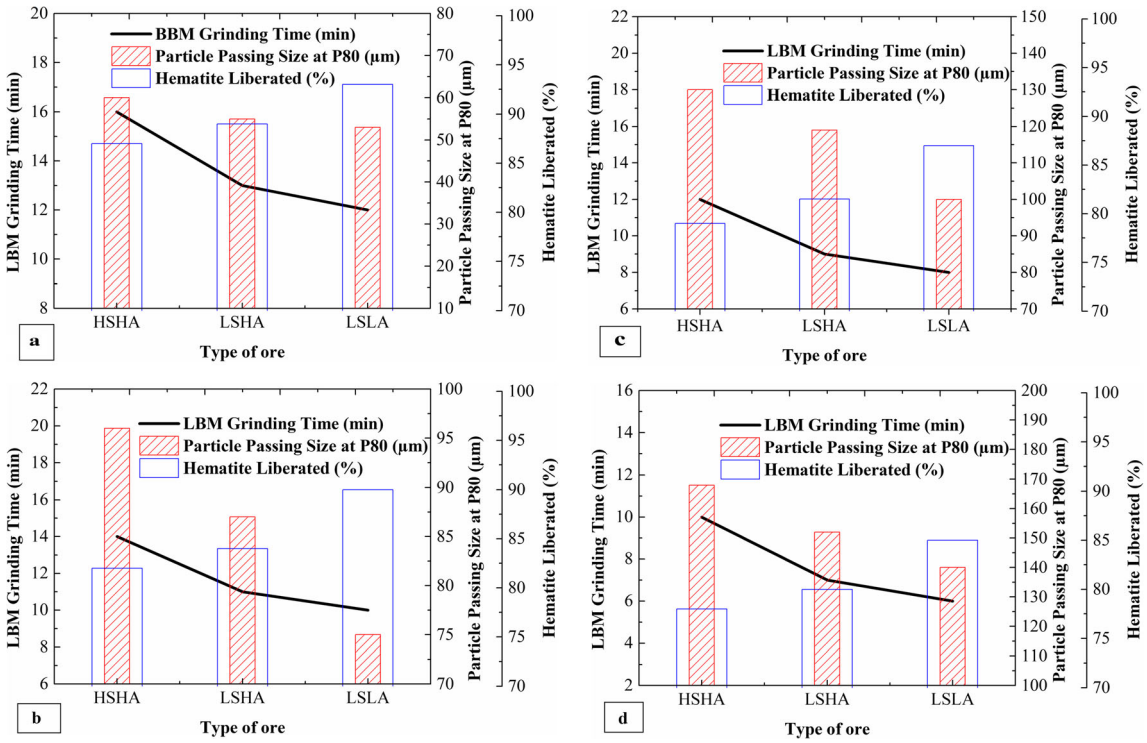

Fig. 13 **a** PSD, percentage of hematite liberation and total grinding time taken for HSHA, LSHA, and LSLA iron ore samples in BBM. **b**–**d** PSD, percentage of hematite liberation and total grinding time taken for HSHA, LSHA, and LSLA iron ore samples ground in LBM

Acknowledgments The present research study is carried out in collaboration between NITK, Surathkal, and JSW Steels, Ballari. The authors are thankful to the management of JSW Steels, Ballari, for their support during the course of this research work. The authors would also like to thank the management of the Partial financial support from Hutti Gold Mines Company Ltd. & Karnataka State Mineral Corporation Ltd. for their partial financial support for this work.

Compliance with Ethical Standards

Conflict of Interest The authors declare that they have no conflict of interest.

References

1. Saeidi N, Noaparast M, Azizi D, Aslani S, Ramadi A (2013) A developed approach based on grinding time to determine ore comminution properties. J Min Environ 4:105–112
2. Narayanan SS, Whiten WJ (1988) Determination of comminution characteristics from single-particle breakage tests and its application to ball-mill scale-up. Trans Inst Min Metall 97:115–124
3. Singh V, Dixit P, Venugopal R, Venkatesh KB (2018) Ore pretreatment methods for grinding: journey and prospects. Miner Process Extr Metall Rev 40:1–15
4. Shi FN, Napier-Munn TJ, Asomah IK (2007) Rheological effects in grinding and classification. Miner Process Extr Metall Rev 20:123–131
5. Rodríguez BÁ, García GG, Coello-Velázquez AL, Menéndez-Aguado JM (2016) Product size distribution function influence on interpolation calculations in the Bond ball mill grindability test. Int J Miner Process 157:16–20
6. Ahmadi R, Shahsavari S (2009) Procedure for determination of ball Bond work index in the commercial operations. Miner Eng 22:104–106
7. Aguado JMM, Velázquez ALC, Tijonov ON, Díaz MAR (2006) Implementation of energy sustainability concepts during the comminution process of the Punta Gorda nickel ore plant (Cuba). Powder Technol 170:153–157
8. Jankovic A, Suthers S, Wills T, Valery W (2015) Evaluation of dry grinding using HPGR in closed circuit with an air classifier. Miner Eng 71:133–138
9. Mosher JB, Tague CB (2001) Conduct and precision of Bond grindability testing. Miner Eng 14:1187–1197
10. Coello Velázquez AL, Menéndez-Aguado JM, Brown RL (2008) Grindability of lateritic nickel ores in Cuba. Powder Technol 182: 113–115
11. Morrell S (2004) An alternative energy-size relationship to that proposed by Bond for the design and optimisation of grinding circuits. Int J Miner Process 74:133–141
12. Magdalinovic N, Trumic M, Trumic G, Magdalinovic S, Trumic M (2012) Determination of the Bond work index on samples of non-standard size. Int J Miner Process 114–117:48–50
13. Tavares LM, De Carvalho RM, Guerrero JC (2012) Simulating the Bond rod mill grindability test. Miner Eng 26:99–101
14. Srivastava MP, Pan SK, Prasad N, Mishra BK (2001) Characterization and processing of iron ore fines of Kiriburu deposit of India. Int J Miner Process 61:93–107
15. Rao SS, Rao DS, Prabhakar S, Raju GB, Kumar TVV (2015) Mineralogy and geochemistry of a low grade iron ore sample from Bellary-Hospet sector, India and their implications on beneficiation. J Miner Mater Charact Eng 08:115–132
16. Angadi SI, Jeon HS, Mohanthy A, Prakash S, Das B (2012) Analysis of wet high-intensity magnetic separation of low-grade Indian iron ore using statistical technique. Sep Sci Technol 47: 1129–1138
17. Rath SS, Dhawan N, Rao DS, Das B (2016) Mishra BK Beneficiation studies of a difficult to treat iron ore using conventional and microwave roasting. Powder Technol 301: 1016–1024
18. Kotake N, Kuboki M, Kiya S, Kanda Y (2011) Influence of dry and wet grinding conditions on fineness and shape of particle-size distribution of product in a ball mill. Adv Powder Technol 22:86–92
19. Mariano RA, Evans CL (2018) The effect of breakage energies on the mineral liberation properties of ores. Miner Eng 126:184–193
20. Engmeermg P. Graphical (1990) Assessment of a random breakage model for mineral liberation. Powder Technol 60:83–97
21. King RP, Schneider CL (1998) Mineral liberation and the batch communition equation. Miner Eng 11:1143–1160
22. Gao P, Yuan S, Han Y, Li Y (2017) Experimental study on the effect of pretreatment with high-voltage electrical pulses on mineral liberation and separation of magnetite ore. Minerals 7:153
23. Dwarapudi S, Devi TU, Mohan Rao S, Ranjan M (2008) Influence of pellet size on quality and microstructure of Iron ore pellets. ISIJ Int 48:768–776
24. Donskoi E, Suthers SP, Fradd SB, Young JM, Campbell JJ, Raynlyn TD, Clout JMF (2007) Utilization of optical image analysis and automatic texture classification for iron ore particle characterisation. Miner Eng 20:461–471
25. Lane GR, Martin C, Pirard E (2008) Techniques and applications for predictive metallurgy and ore characterization using optical image analysis. Miner Eng 21:568–577
26. Sutherland DN, Gottlieb P (1991) Application of automated quantitative mineralogy in mineral processing. Miner Eng 4:753–762
27. Devasahayam S (2015) Predicting the liberation of sulfide minerals using the breakage distribution function. Miner Process Extr Metall Rev 36:136–144
28. Hagni AM (2008) Phase identification, phase quantification, and phase association determination utilizing automated mineralogy technology. Jom 60:33–37
29. Hoal KO, Stammer JG, Appleby SK, Botha J, Ross JK, Botha PW (2009) Research in quantitative mineralogy: examples from diverse applications. Miner Eng 22:402–408
30. Hassanzadeh A, Hassanzadeh A (2018) A new statistical view to modeling of particle residence time distribution in full-scale overflow ball mill operating in closed-circuit. Geosystem Eng 9328:1–11
31. Cho H, Austin LG (2002) The equivalence between different residence time distribution models in ball milling. Powder Technol 124:112–118
32. Mulenga FK, Chimwani N (2013) Introduction to the use of the attainable region method in determining the optimal residence time of a ball mill. Int J Miner Process 125:39–50
33. Chimwani N, Mulenga FK, Hildebrandt D, Glasser D, Bwalya MM (2015) Use of the attainable region method to simulate a full-scale ball mill with a realistic transport model. Miner Eng 73:116–123
34. Gupta VK, Patel JP (2015) A one-parameter model for describing the residence time distribution of closed continuous flow systems characterized by nonlinear reaction kinetics : rod and ball mills. Powder Technol 274:163–172
35. Vinnett L, Contreras F, Lazo A, Morales M, Díaz F, Waters KE (2018) The use of radioactive tracers to measure mixing regime in semi-autogenous grinding mills. Miner Eng 115:41–43

36. Vizcarra TG, Wightman EM, Johnson NW, Manlapig EV (2010) The effect of breakage mechanism on the mineral liberation properties of sulphide ores. Miner Eng 23:374–382
37. Chapman NA, Shackleton NJ, Malysiak V, O'Connor CT (2011) The effect of using different comminution procedures on the flotation of platinum-group minerals. Miner Eng 24:731–736
38. Solomon N, Becker M, Mainza A, Petersen J, Franzidis J (2011) Understanding the influence of HPGR on PGM flotation behavior using mineralogy. Miner Eng 24:1370–1377
39. Gilvarry JJ, Bergstrom BH (1961) Fracture of brittle solids. I. Distribution function for fragment size in single fracture (experimental). J Appl Phys 32:400–410
40. Bond FC (1960) Crushing and grinding calculations. Br Chem Eng 80:543–548
41. Liu L, Tan Q, Liu L, Cao J (2018) Comparison of different comminution flow sheets in terms of minerals liberation and separation properties. Miner Eng 125:26–33